

# Mechanical Behavior of Carbonate Rocks at Crack Damage Stress Equal to Uniaxial Compressive Strength

V. Palchik

Received: 8 January 2009 / Accepted: 5 March 2009 / Published online: 19 March 2009  
© Springer-Verlag 2009

## 1 Introduction

A number of researchers such as Brace et al. (1966), Bieniawski (1967), Brady and Brown (1993), Martin and Chandler (1994), Hatzor and Palchik (1997), Pettitt et al. (1998), Eberhardt et al. (1999), Katz and Reches (2004) and Cai et al. (2004) have investigated different stages of stress-strain behavior of brittle rocks during uniaxial compression. Two stress-strain diagrams in Fig. 1 obtained by the author for carbonate rocks, exhibit three main characteristic stress levels (crack initiation stress  $\sigma_{ci}$ , crack damage stress  $\sigma_{cd}$  and uniaxial compressive strength  $\sigma_c$ ) which are represented by points A, B and C, respectively, over the total volumetric strain curve. The crack initiation stress ( $\sigma_{ci}$ , point A) is the stress level at which microfracturing begins. The point A is the end of the elastic stage (linear portion) of stress-strain curve. The crack damage stress ( $\sigma_{cd}$ , point B) is the stress at the onset of dilation: when  $\sigma_{cd}$  is attained, the rock volume begins to increase (Schock et al. 1973; Brace 1978; Paterson 1978; Palchik and Hatzor 2002). The crack damage stress ( $\sigma_{cd}$ , point B) is the stress level at which maximum total volumetric strain ( $\varepsilon_{cd}$ ) is attained. The uniaxial compressive strength ( $\sigma_c$ , point C) is the maximum axial stress (at failure). In Fig. 1, strain  $\varepsilon_{cd}$  at  $\sigma_{cd}$  (point B) is the maximum total volumetric strain, and strain  $\varepsilon_{a\ max}$  at  $\sigma_c$  is the maximum axial strain.

Martin and Chandler (1994), Eberhardt et al. (1999) and Palchik and Hatzor (2002) have shown that the crack

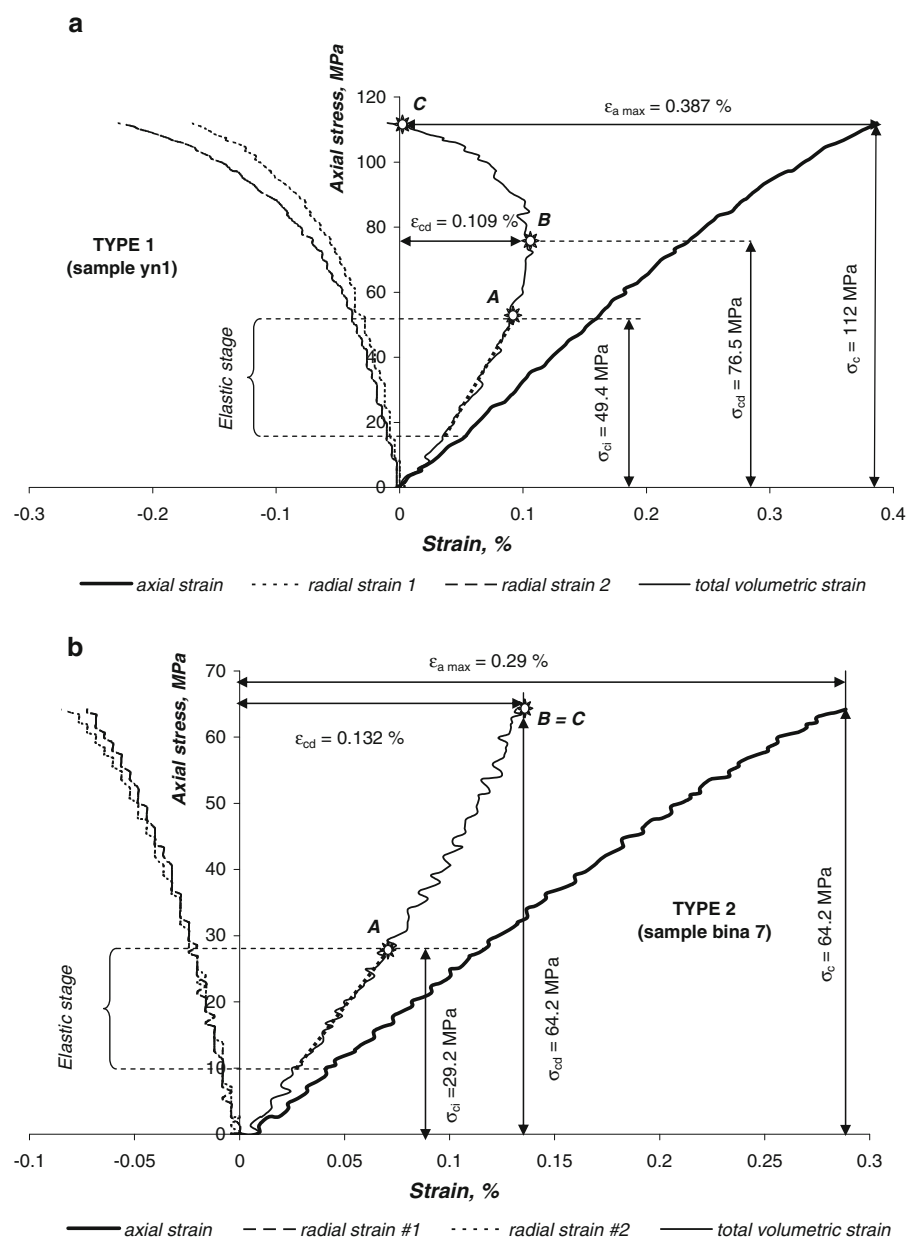
damage stress ( $\sigma_{cd}$ ) is defined as the point (see point B in Fig. 1a) where a total volumetric strain reversal occurs and unstable crack growth begins. In this case (see Fig. 1a), crack damage stress  $\sigma_{cd}$  is lower than the uniaxial compressive strength ( $\sigma_c$ ). Indeed, Brace et al. (1966), Bieniawski (1967), Martin (1993), Pettitt et al. (1998), Eberhardt et al. (1999), Heo et al. (2001) and Katz and Reches (2004) have found that the crack damage stresses  $\sigma_{cd}$  of granites, sandstones and quartzite vary from  $0.71\sigma_c$  to  $0.84\sigma_c$ . They have also shown that the ratios  $\sigma_{ci}/\sigma_c$  and  $\sigma_{ci}/\sigma_{cd}$  for above-mentioned rocks range from 0.39 to 0.6 and from 0.52 to 0.82, respectively.

Hatzor and Palchik (1997) and Palchik and Hatzor (2002) have shown that there exist total volumetric strain curves (in heterogeneous carbonate rocks) which do not have any point of reversal, with the maximum total volumetric strain ( $\varepsilon_{cd}$ ) attained at the uniaxial compressive strength ( $\sigma_c$ ). In this case, crack damage stress is equal to uniaxial compressive strength (i.e.  $\sigma_{cd} = \sigma_c$ , B = C in Fig. 1b). Thus, there are two types of total volumetric strain curves in brittle rocks: type 1 (see Fig. 1a), with a point of reversal (B) in the total volumetric strain curve, and  $\sigma_{cd} < \sigma_c$ ; and type 2 (see Fig. 1b), where the total volumetric strain curve has no reversal point and, therefore,  $\sigma_{cd} = \sigma_c$ .

Type 1 (Fig. 1a) curves have been studied by Brace et al. (1966), Bieniawski (1967), Pettitt et al. (1998), Eberhardt et al. (1999), Heo et al. (2001), Katz and Reches (2004), etc., whereas little attention has been paid to type 2 mechanical behavior of brittle rocks (Fig. 1b). In this paper, we intend to study relations between characteristic compressive stress levels, strains and mechanical properties of heterogeneous carbonate rocks exhibiting type 2 behavior of the total volumetric strain curve (i.e. at  $\sigma_{cd} = \sigma_c$ ).

V. Palchik (✉)  
Department of Geological and Environmental Sciences,  
Ben-Gurion University of the Negev, P.O. Box 653,  
84105 Beer-Sheva, Israel  
e-mail: vplachek@bgu.ac.il

**Fig. 1** Stress-strain behavior of brittle rocks during uniaxial compression. Crack initiation stress ( $\sigma_{ci}$ ), crack damage stress ( $\sigma_{cd}$ ) and uniaxial compressive strength ( $\sigma_c$ ) are represented by points A, B and C, respectively. The total volumetric strain ( $\varepsilon_v$ ) is calculated as a sum of the component strains:  $\varepsilon_v = \varepsilon_a + \varepsilon_{R1} + \varepsilon_{R2}$ , where  $\varepsilon_a$  is axial strain, and  $\varepsilon_{R1}$  and  $\varepsilon_{R2}$  are radial strains measured in orthogonal directions (Palchik and Hatzor 2002): **a** type 1—total volumetric strain curve has a reversal point (B) and  $\sigma_{cd} < \sigma_c$ ; **b** type 2—there is no reversal point in total volumetric strain curve, and  $\sigma_{cd} = \sigma_c$



## 2 Testing and test results

Mechanical properties of carbonate rock samples exhibiting type 2 behavior of the total volumetric strain curve are summarized in Table 1. These samples were collected from Adulam chalk, Aminadav dolomite, Bina limestone, Yarka limestone, Yagur dolomite, and Nekorot limestone formations. The NX ( $d = 54$  mm) sized cylindrical rock samples having the ratio  $L/d = 2$  (here  $L$  and  $d$  are the length and diameter of a sample, respectively) were prepared. The samples were ground to the planeness of 0.01 mm and cylinder perpendicularity within 0.05 radians. Prior to testing, rock samples were oven dried at the temperature of 110°C for 24 h.

Uniaxial compressive tests were performed at the Rock Mechanics Laboratory of the Ben-Gurion University. The tests were conducted using a load frame (TerraTek system, model FX-S-33090) at a constant strain rate of  $10^{-5}/s$ . The load frame operates under a hydraulic closed-loop servo-control. The load frame stiffness and maximum axial force are  $5 \times 10^9$  N/m and 1.4 MN, respectively. The axial strain cantilever set has a 10% strain range, and the radial strain cantilevers have a strain range limit of 7%, with the linearity of 1% over the full scale in both sets. The servo-controlled press description, physical and mechanical properties of the studied rock formations are presented in detail elsewhere (Hatzor and Palchik 1997; Palchik and Hatzor 2002, 2004).

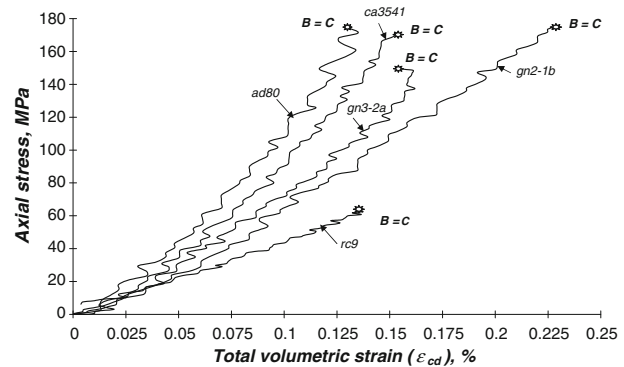
**Table 1** Observed values of compressive stress levels, elastic modulus, dry bulk density, Poisson's ratio, porosity, maximum axial strain and maximum total volumetric strain

Rock form	Sample	$\sigma_{ci}$ (MPa)	$\sigma_{cd} = \sigma_c$ (MPa)	E (MPa)	$\rho$ (g/cm <sup>3</sup> )	$\nu$	n (%)	$\varepsilon_{a\ max}$ (%)	$\varepsilon_{cd}$ (%)
AD	rc1	40.1	53.2	17,400	2.12	0.23	21.5	0.32	0.16
	rc3	29.3	51	16,000	2.07	0.26	23.3	0.41	0.229
	rc4	15	31.9	11,700	1.93	0.2	28.5	0.32	0.166
	rc8	30.9	60.3	17,300	2.11	0.2	21.9	0.37	0.218
	rc9	49.4	63.1	20,500	2.17	0.27	19.6	0.31	0.134
	st2a	29.6	52.3	14,300	2.14	0.2	20.7	0.4	0.186
	st2b	25.5	37.4	10,700	2.06	0.22	23.7	0.34	0.159
AM	ad 43	145	274	64,000	2.65	0.27	5.4	0.475	0.21
	ad 80	102	174	58,500	2.62	0.28	6.4	0.316	0.134
BIN	bina 2	41.7	77	34,400	2.36	0.25	15.7	0.317	0.136
	bina 5	49.7	80	38,700	2.41	0.24	13.9	0.22	0.1
	bina 7	29.2	64.2	25,000	2.4	0.2	14.3	0.29	0.132
	tb3-2	89.2	139	42,830	2.59	0.26	7.5	0.362	0.147
	b3	22.2	35	21,000	2.06	0.31	26.4	0.19	0.084
	b5	65.9	98	35,200	2.33	0.25	16.8	0.29	0.137
	Yark 3	29.8	41	6,200	2.3	0.18	17.9	0.69	0.312
YG	yn 4	45.2	75	6,100	2.1	0.13	25	1.36	0.9
	ca3541	110	174	54,000	2.57	0.19	8.2	0.346	0.149
NK	ca5671	39.5	60	35,500	2.33	0.19	16.8	0.232	0.14
	gn2-1b	80	177	47,000	2.48	0.23	11.4	0.431	0.236
	gn2-4a	100	141	44,600	2.43	0.25	13.2	0.33	0.165
	gn2-5b	121.5	162	48,600	2.49	0.25	11.1	0.364	0.197
	gn3-2a	90.5	150	44,800	2.45	0.24	12.5	0.361	0.161
	gn3-2c	99	163	44,400	2.42	0.25	13.6	0.395	0.186

AD Adulam chalk, AM Aminadav dolomite, BIN Bina limestone, YR Yarka limestone, YG Yagur dolomite, NK Nekorot limestone,  $\sigma_{ci}$  crack initiation stress,  $\sigma_{cd}$  crack damage stress,  $\sigma_c$  uniaxial compressive strength, E elastic modulus,  $\rho$  dry bulk density,  $\nu$  Poisson's ratio, n porosity,  $\varepsilon_{a\ max}$  maximum axial strain (at  $\sigma_c$ ),  $\varepsilon_{cd}$  maximum total volumetric strain (at  $\sigma_{cd}$ )

The results of uniaxial tests are given in Table 1. The latter presents the values of crack initiation stress ( $\sigma_{ci}$ ),  $\sigma_{cd} = \sigma_c$  (here  $\sigma_{cd}$  is the crack damage stress and  $\sigma_c$  is the uniaxial compressive strength), elastic modulus (E), dry bulk density ( $\rho$ ), Poisson's ratio ( $\nu$ ), porosity (n), maximum axial strain  $\varepsilon_{a\ max}$  (at  $\sigma_c$ ) and maximum total volumetric strain  $\varepsilon_{cd}$  (at  $\sigma_{cd}$ ) for each of 24 studied rock samples.

Porosity (n, %) was calculated from the measured values of dry bulk density ( $\rho$  in Table 1) and specific gravity of the solids ( $G_s = 2.7\text{--}2.8\text{ g/cm}^3$ ):  $n = [1 - (\rho/G_s)] \times 100\%$ . The precision of the porosity estimation is 0.1%. The elastic modulus (E) and Poisson's ratio ( $\nu$ ) were calculated using linear regressions along the linear portion (elastic stage) of the stress-strain curve. The total volumetric strains ( $\varepsilon_v$ ) calculated as a sum of the component strains ( $\varepsilon_a$ ,  $\varepsilon_{R1}$  and  $\varepsilon_{R2}$ ) were plotted versus axial stresses for each of 24 studied rock samples. Figure 2 demonstrates examples of axial stress–total volumetric strain curves for five rock samples (ad 80, ca3541, gn3-2a, gn2-1b and rc9) exhibiting  $\varepsilon_{cd} = 0.134\%$  at  $\sigma_{cd} = \sigma_c = 177\text{ MPa}$ ,  $\varepsilon_{cd} = 0.149\%$  at  $\sigma_{cd} = \sigma_c = 174\text{ MPa}$ ,  $\varepsilon_{cd} = 0.161\%$  at  $\sigma_{cd} = \sigma_c = 150\text{ MPa}$ ,

**Fig. 2** Examples of observed axial stress–total volumetric strain curves (type 2) for five studied rock samples

$\varepsilon_{cd} = 0.236\%$  at  $\sigma_{cd} = \sigma_c = 177\text{ MPa}$  and  $\varepsilon_{cd} = 0.134\%$  at  $\sigma_{cd} = \sigma_c = 63.1\text{ MPa}$ , respectively, in point the  $B = C$ .

In Table 1, the observed values of crack initiation stress ( $\sigma_{ci}$ ) and crack damage stress or uniaxial compressive strength ( $\sigma_{cd} = \sigma_c$ ) vary from 15 to 145 MPa with the

mean of 61.7 MPa and from 31.9 to 273.9 MPa with the mean of 101.4 MPa, respectively. The difference ( $D$ ) between  $\sigma_c$  and  $\sigma_{ci}$  and the ratio  $k = \sigma_{ci}/\sigma_c$  for each of the studied rock samples were calculated. Values of  $D$  and  $k$  range from 11.2 to 128.9 MPa ( $D_{mean} = 39.7$  MPa) and from 0.45 to 0.78 ( $k_{mean} = 0.62$ ), respectively, for all studied samples. Here, standard deviations ( $\Delta$ ) of the mean  $D$  and  $k$  values are significant—29.2 MPa and 0.09, respectively. Standard deviation of the mean has been calculated as follows:

$$\Delta = \sqrt{\frac{\sum_{i=1}^n (q_i - q_m)^2}{n-1}} \quad (1)$$

where  $i = 1, 2, \dots, n$  is the number of observed sample ( $n = 24$ ),  $q_i$  is the value of the observed parameter ( $D$  or  $k$ ) in the  $i$ th sample,  $q_m$  is the arithmetic mean of parameters observed in  $n$  samples.

Note also that the values of  $D$  and  $k$  are not constant even for a single set of samples within the same rock formation:  $11.9 \text{ MPa} < D < 29.4 \text{ MPa}$  ( $0.47 < k < 0.78$ ),  $72.2 \text{ MPa} < D < 128.9 \text{ MPa}$  ( $0.53 < k < 0.59$ ),  $12.8 \text{ MPa} < D < 49.8 \text{ MPa}$  ( $0.47 < k < 0.63$ ),  $20.5 \text{ MPa} < D < 63.9 \text{ MPa}$  ( $0.6 < k < 0.66$ ) and  $40.5 \text{ MPa} < D < 97 \text{ MPa}$  ( $0.45 < k < 0.75$ ) for Adulam chalk, Aminadav dolomite, Bina limestone, Yagur dolomite and Nekorot limestone, respectively. The standard deviation ( $\Delta$ ) of the mean  $k$  within the same rock formation ranges from 0.03 to 0.12. For example, Nekorot limestone has a large  $\Delta k = 0.12$ , whereas Yagur dolomite exhibits relatively a small  $\Delta k = 0.03$ .

Table 1 demonstrates the values of elastic modulus ( $E$ ), porosity ( $n$ ) and Poisson's ratio ( $v$ ) for each of 24 studied rock samples. Here,  $6,100 \text{ MPa} < E < 64,000 \text{ MPa}$ ,  $5.4\% < n < 28.5\%$  and  $0.13 < v < 0.31$ . Mean values of  $E$ ,  $n$  and  $v$  are  $31,600 \text{ MPa}$ ,  $16.5\%$  and  $0.23$ , respectively, and standard deviations ( $\Delta$ ) of mean  $E$ ,  $n$  and  $v$  values are  $17,300 \text{ MPa}$ ,  $6.5\%$  and  $0.04$ , respectively. The values of  $E$ ,  $n$  and  $v$  in heterogeneous carbonate rocks are also non-constant even for samples within the same rock formation. For example, Bina limestone exhibits  $21,000 \text{ MPa} < E < 42,830 \text{ MPa}$ ,  $7.5\% < n < 26.4\%$  and  $0.2 < v < 0.31$ .

In Table 1, maximum total volumetric strain ( $\varepsilon_{cd}$ ) and maximum axial strain ( $\varepsilon_{a max}$ ) range from 0.084 to 0.9% with the mean of 0.2% and from 0.19 to 1.36% with the mean of 0.39%, respectively. Thus, the maximum axial strain ( $\varepsilon_{a max}$ ) is 1.5–2.5 times larger than the maximum total volumetric strain ( $\varepsilon_{cd}$ ) in case where crack damage stress ( $\sigma_{cd}$ ) is equal to uniaxial compressive strength ( $\sigma_c$ ). For example, rock sample bina 7 exhibiting  $\varepsilon_{cd} = 0.132\%$  at  $\sigma_{cd} = 64.2 \text{ MPa}$  and  $\varepsilon_{a max} = 0.29\%$  at  $\sigma_c = 64.2 \text{ MPa}$  (see Fig. 1b), has the ratio  $\varepsilon_{a max}/\varepsilon_{cd} = 0.29/0.132 = 2.2$ .

### 3 Relations between mechanical properties and compressive stresses

#### 3.1 Effect of elastic modulus, porosity and $E/n$ ratio on $\sigma_{ci}$ and $\sigma_{cd} = \sigma_c$

Figure 3a shows how the elastic modulus ( $E$ ) influences the values of  $\sigma_{ci}$  and  $\sigma_{cd} = \sigma_c$ . Relations  $\sigma_{ci} - E$  and  $\sigma_c - E$  best follow a polynomial law with good squared regression coefficients  $R^2 = 0.86$  and  $0.91$  for  $\sigma_{ci} - E$  and  $\sigma_c - E$ , respectively. An increase in the elastic modulus ( $E$ ) from 6,100 to 64,000 MPa leads to an increase in  $\sigma_{ci}$  and  $\sigma_c = \sigma_c$  values from 15 to 145 MPa and from 31.9 to 273.9 MPa, respectively. Hence, an increase in the elastic modulus by a factor of 10.5 leads to an increase in the values of  $\sigma_{ci}$  and  $\sigma_{cd} = \sigma_c$  by a factor of 9.7 and 8.6, respectively.

On the other hand, values of  $\sigma_{ci}$  decrease from 145 to 15 MPa and from 273.9 to 31.9 MPa, respectively, with porosity increase ( $n$ , Fig. 3b) from 5.4 to 28.5%. In Fig. 3b, polynomial correlations ( $R^2 = 0.76$ –0.79) between the porosity ( $n$ ) and  $\sigma_{ci}$  and  $\sigma_{cd} = \sigma_c$  values are obtained.

An increase in the values of stresses  $\sigma_{ci}$  and  $\sigma_{cd} = \sigma_c$  with increasing ratio  $E/n$  is shown in Fig. 4a. The latter demonstrates that  $\sigma_{ci}$  and  $\sigma_{cd} = \sigma_c$  are well correlated ( $R^2 = 0.82$ –0.86) with the ratio  $E/n$ . It is not surprising, since the compressive stresses  $\sigma_{ci}$  and  $\sigma_{cd} = \sigma_c$  depend on the elastic modulus  $E$  (Fig. 3a) and porosity  $n$  (Fig. 3b).

#### 3.2 Effect of $E/\lambda$ ratio on $\sigma_{ci}$ and $\sigma_{cd} = \sigma_c$

Porosity  $n$  is a measure of void space (pores and open cracks) and represents a ratio between the void space ( $V_p$ ) and bulk volume ( $V$ ).

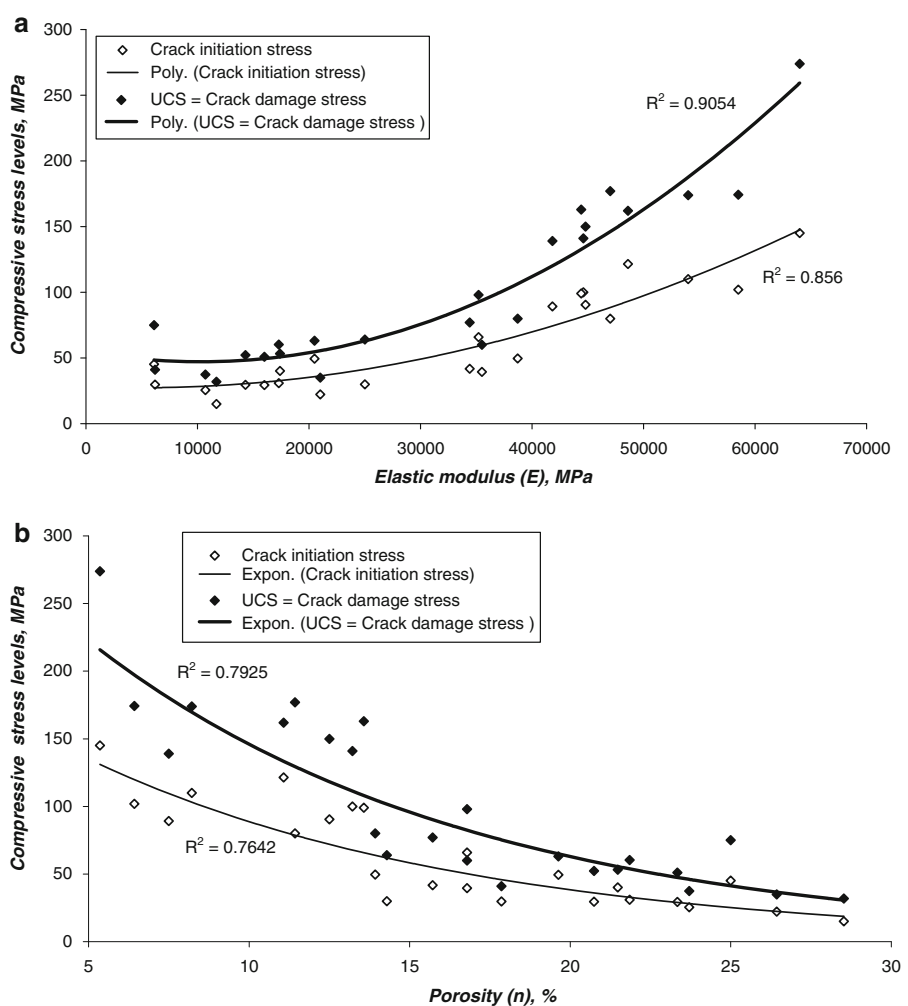
$$n = \frac{V_p}{V} \quad (2)$$

The bulk volume ( $V$ ) is the initial volume of a sample before loading, and therefore, it does not reflect the change in the volume due to compression. Palchik and Hatzor (2002) have proposed to use the ratio between the volume of voids and change in the bulk volume due to compression, since such ratio reflects the mechanical behavior of the rock matrix. This ratio can be represented as a ratio between the volume of voids ( $V_p$ ) and the maximum compaction ( $V_c$ ) of a rock sample:

$$\lambda = \frac{V_p}{V_c} \quad (3)$$

where  $V_c$  is the maximum decrease in a sample volume (maximum compaction of a sample), which is attained at the maximum total volumetric strain  $\varepsilon_{cd}$  (at crack damage stress  $\sigma_{cd}$ ).

**Fig. 3** Relations between compressive stress levels and **a** elastic modulus ( $E$ ), and **b** porosity ( $n$ )



The parameter  $\lambda$  can be presented as

$$\lambda = \frac{V_p}{V_c} = \frac{V_p}{V} / \frac{V_c}{V} = \frac{n}{\varepsilon_{cd}} \quad (4)$$

where  $V_c/V = \varepsilon_{cd}$ ,  $\varepsilon_{cd}$  is the maximum total volumetric strain at the crack damage stress  $\sigma_{cd}$ .

When we use  $\lambda = V_p/V_c$  instead of  $n = V_p/V$ , the ratio  $E/n$  can be rewritten as  $E/\lambda$ . Relations between  $E/\lambda$  and compressive stress levels are presented in Fig. 4b. From Fig. 4b it is clear that the values of  $\sigma_{cd} = \sigma_c$  and  $D = \sigma_c - \sigma_{ci}$  are well correlated with  $E/\lambda$ . Here, power dependences between  $\sigma_{cd} = \sigma_c$  ( $R^2 = 0.96$ ),  $D$  ( $R^2 = 0.87$ ) and  $E/\lambda$  with good squared regressions coefficients  $R^2$  are obtained:

$$\sigma_{cd} = \sigma_c = a \left( \frac{E}{\lambda} \right)^b \quad (5)$$

$$D = c \left( \frac{E}{\lambda} \right)^d \quad (6)$$

where coefficients  $a = 2.75$ ,  $b = 0.6$ ,  $c = 0.82$  and  $d = 0.64$ .

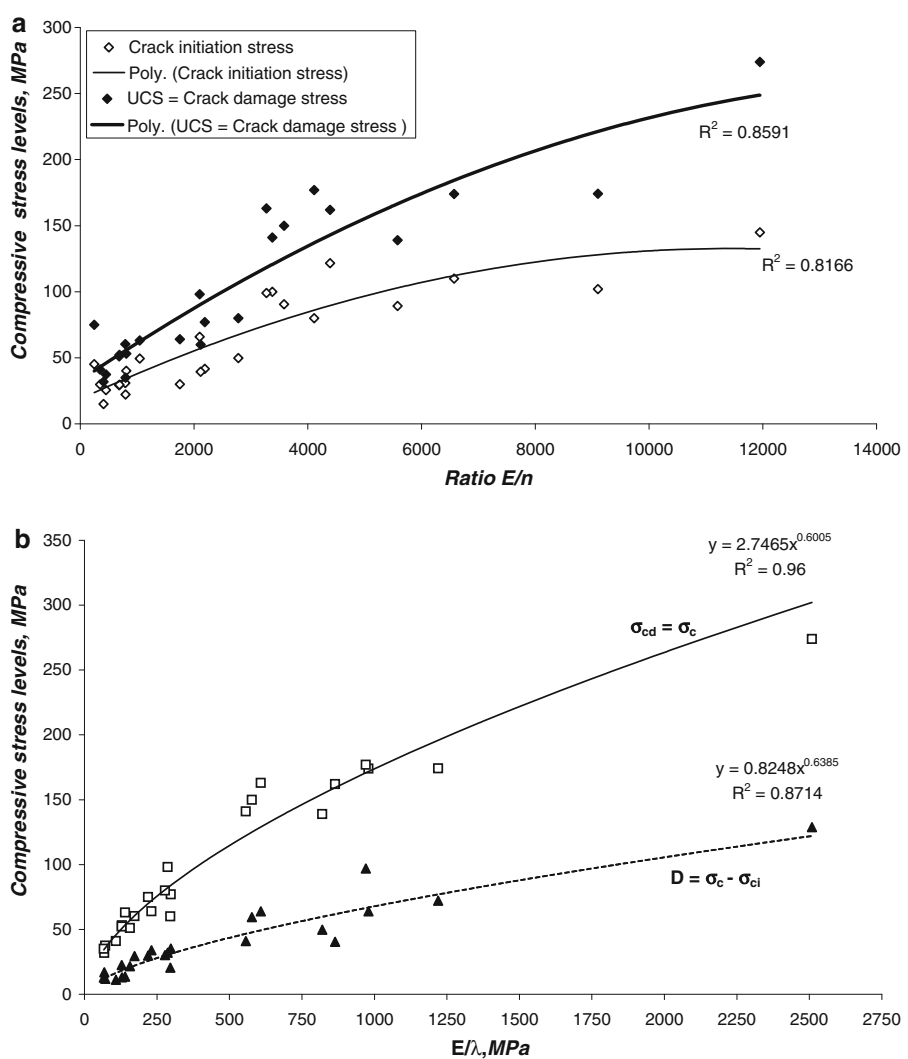
Note that the use of  $E/\lambda$  ratio (Fig. 4b) instead of  $E/n$  (Fig. 4a) versus the compressive stress  $\sigma_{cd} = \sigma_c$  allows us to increase the value of  $R^2$  from 0.86 to 0.96. Hence, the effect of the ratio  $E/\lambda$  on uniaxial compressive strength ( $\sigma_c$ ) is more pronounced than the effect of  $E/n$ .

#### 4 Conclusions

The mechanical behavior of heterogeneous carbonate rocks exhibiting total volumetric strain curves of type 2 was studied. Studied rock samples exhibiting a wide range of mechanical properties ( $31.9 \text{ MPa} < \sigma_{cd} = \sigma_c < 273.9 \text{ MPa}$ ,  $6,100 \text{ MPa} < E < 64,000 \text{ MPa}$  and  $5.4\% < n < 28.5\%$ ) were collected from different geological settings of Israel. From the results of this study it can be concluded that:

- Crack initiation (at the crack initiation stress  $\sigma_{ci}$ ) for studied heterogeneous carbonate rocks occurs at  $0.45\sigma_c/0.78\sigma_c$  (at significant standard deviations  $\Delta D = 29.2 \text{ MPa}$  and  $\Delta k = 0.09$  for all studied samples).

**Fig. 4** Relations between compressive stress levels and ratios **a**  $E/n$  and **b**  $E/\lambda$



- Values of the difference ( $D$ ) between the uniaxial compressive strength and crack initiation stress, and the ratio ( $k$ ) between the crack initiation stress and uniaxial compressive strength are not constant even for samples within the same rock formation. The standard deviation ( $\Delta$ ) of the mean  $k$  within the same rock formation varies between 0.03 and 0.12.
- Values of the maximum axial strain ( $\varepsilon_{a \max}$ ) and maximum volumetric strain ( $\varepsilon_{cd}$ ) at  $\sigma_{cd} = \sigma_c$  are 0.19/1.36% and 0.084/0.9%, respectively. At  $\sigma_{cd} = \sigma_c$ , the maximum axial strain ( $\varepsilon_{a \ max}$ ) is 1.5–2.5 times the maximum volumetric strain ( $\varepsilon_{cd}$ ).
- The ratio between the elastic modulus ( $E$ ) and parameter  $\lambda$  strongly influences the values of  $\sigma_{cd} = \sigma_c$  and  $D = \sigma_c - \sigma_{ci}$ . Power dependencies between  $\sigma_{cd} = \sigma_c$ ,  $\sigma_c - \sigma_{ci}$  and  $E/\lambda$  are obtained. Parameter  $\lambda$  is a ratio between the volume of voids ( $V_p$ ) and the maximum compaction ( $V_c$ ) of rock sample. Parameter  $\lambda$  is

calculated as  $n/\varepsilon_{cd}$ , where  $\varepsilon_{cd}$  is the maximum total volumetric strain.

## References

- Bieniawski ZT (1967) Mechanism of brittle fracture of rock. *Int J Rock Mech Min Sci* 4(4):395–430
- Brace WF (1978) Volume changes during fracture and frictional sliding: a review. *PAGEOGH* 116:603–614
- Brace WF, Paulding B, Scholz C (1966) Dilatancy in the fracture of crystalline rocks. *J. Geoph Res* 71(16):3939–3953
- Brady BHG, Brown ET (1993) Rock mechanics for underground mining, 2nd edn. Chapman and Hall, London, p 571
- Cai M, Kaiser PK, Tasaka Y, Maejima T, Morioka H, Minami M (2004) Generalized crack initiation and crack damage stress thresholds of brittle rock masses near underground excavations. *Int J Rock Mech Min Sci* 41(5):833–847
- Eberhardt E, Stead D, Stimpson B (1999) Quantifying progressive pre-peak brittle fracture damage in rock during uniaxial compression. *Int J Rock Mech Min Sci* 36:361–380

- Hatzor YH, Palchik V (1997) The influence of grain size and porosity on crack initiation stress and critical flaw length in dolomites. *Int J Rock Mech Min Sci* 34(5):805–816
- Heo JS, Cho HK, Lee CI (2001) Measurement of acoustic emission and source location considering anisotropy of rock under triaxial compression. In: Sarkka P, Eloranta P (eds) *Rock mechanics a challenge for society*. Swets & Zeitlinger Lisse, Espoo, Finland, pp 91–96
- Katz O, Reches Z (2004) Microfracturing, damage and failure of brittle granites. *J Geophys Res* 109(B1)
- Martin CD (1993) Strength of massive Lac du Bonnet granite around underground openings. PhD thesis, Department of Civil and Geological Engineering, University of Manitoba, Winnipeg
- Martin CD, Chandler NA (1994) The progressive fracture of Lac du Bonnet Granite. *Int J Rock Mech Min Sci* 31(6):643–659
- Palchik V, Hatzor YH (2002) Crack damage stress as a composite function of porosity and elastic matrix stiffness in dolomites and limestones. *Eng Geol* 63(3–4):233–245
- Palchik V, Hatzor YH (2004) The influence of porosity on tensile and compressive strength of porous chalks. *Rock Mech Rock Engng* 37(4):331–341
- Paterson MS (1978) Experimental rock deformation—the brittle field. Springer, New York, p 254
- Pettitt WS, Young RP, Marsden JR (1998) Investigating the mechanics of microcrack damage induced under true-triaxial unloading. In: Eurock 98. Society of Petroleum Engineering, p SPE 47319
- Schock RN, Heard HC, Stevens DR (1973) Stress-strain behavior of a granodiorite and two graywackes on compression to 20 kilobars. *J Geophys Res* 78:5922–5941